**Science and Technology Indonesia**
*e*-ISSN:2580-4391 *p*-ISSN:2580-4405
Vol. 7, No. 4, October 2022

Research Paper

# Green Synthesis of Nickel Aluminum Layered Double Hydroxide using Chitosan as Template for Adsorption of Phenol

Hasja Paluta Utami[1], Nur Ahmad[2], Zaqiya Artha Zahara[3], Aldes Lesbani[2,4], Risfidian Mohadi[1,4]*

[1]*Magister Programme Graduate School of Mathematics and Natural Sciences, Sriwijaya University, Palembang, South Sumatera, 30139, Indonesia*
[2]*Graduate School of Mathematics and Natural Sciences, Faculty of Mathematics and Natural Sciences, Sriwijaya University, Palembang, South Sumatera, 30139, Indonesia*
[3]*Magister Programme in Environment Management, Sriwijaya University, Palembang, South Sumatera, 30139, Indonesia*
[4]*Research Center of Inorganic Materials and Coordination Complexes, Faculty of Mathematics and Natural Sciences, Sriwijaya University, Palembang, South Sumatera, 30139, Indonesia*
***Corresponding author**: risfidian.mohadi@unsri.ac.id

**Abstract**
In present study, a modification of the NiAl LDH composite with chitosan was successful. Characterization was carried out using X-rays, The results obtained show that there is an angle of 2$\theta$ at 11.57°(003); 22.91°(006); 35.04°(012); 39.73°(015); and 61.9°(110). The FT-IR spectrum of the Chitosan@NiAl LDH at Wavenumber 3448, 1635, 1543, and 601 $cm^{-1}$. The NiAl LDH and chitosan have a surface area of 3.288 $m^2$/g and 8.558 $m^2$/g, respectively. An increase in the surface area of the composite Chitosan@NiAl LDH 9.493 $m^2$/g, all of adsorbents follow type IV isotherm based on the classification according to IUPAC. The optimum pH of the NiAl LDH at pH 3. The optimum pH for chitosan and chitosan@NiAl LDH material is at the optimum pH of 5. The kinetic and isotherm model in the adsorption process is pseudo-second-order and Freundlich model, respectively. The maximum adsorption capacity of NiAl LDH, chitosan, and chitosan@NiAl LDH is 25.445, 23.753, and 33.223 mg/g, respectively. The increase in regeneration cycles causes a decrease in the percentage of adsorbed; sequentially, the percentage adsorbed during the fifth regeneration reaches 3.545, 1.966, 4.309%, respectively.

**Keywords**
Layered Double Hydroxide, Chitosan, Phenol, Adsorption

Received: 15 August 2022, Accepted: 24 October 2022
https://doi.org/10.26554/sti.2022.7.4.530-535

## 1. INTRODUCTION

Along with the increasing population and technological developments, water pollution is one of the severe problems faced and has become a concern of many parties. One of the harmful pollutants in the environment is phenol (Alves et al., 2019). Phenol waste can come from production processes in various industries such as metal smelting, plastics, polymers, pharmaceuticals, paints, wood processing, organic pesticides, pulp, and paper (Dehmani et al., 2021b; Wang et al., 2022; Zhang et al., 2022).

The presence of phenol in the environmenst, especially waters, can disrupt aquatic ecosystems and human health (da Silva et al., 2022). United State Environmental Agency (USEPA) has limit concentration of phenol in water is 1 $\mu$g/L (de Farias et al., 2022). Therefore, to overcome the problem of environmental pollution, a solution is needed, one of which is the adsorption method (Khan et al., 2022). Adsorption has several advantages compared to other methods, including the relatively straightforward process, relatively high effectiveness, and efficiency (Jain et al., 2022).

The adsorbent dramatically determines the success of the adsorption process, which is characterized by a large adsorption capacity. Researchers have used many adsorbents to overcome environmental pollution problems, such as humic acid, zeolite, clay, activated carbon, chitosan, and layered double hydroxide (Lesbani et al., 2021). Layered double hydroxide (LDH) is an anionic clay material and hydrotalcite with the ability to exchange ions between layers, which has the general formula $[M^{2+}{}_{1-x}M^{3+}{}_{x}(OH)_2]^{x+}[(A^{n-})_{x/n}{\cdot}yH_2O]^{x-}$, where M is divalent and trivalent metal cations (Bouteraa et al., 2020). Layered double hydroxides have been widely developed into adsorbents because they have good adsorption and uniqueness (Taher et al., 2021).

The development of LDH composites was also carried out on a hydrochar basis. Research by Juleanti et al. (2022) compared the adsorption ability of Mg/Al, Ca/Al, and Zn/Al composites based on hydrochar on the absorption of direct

green dyes. The ability of these hydrochar-based composites to have adsorption capacities of 94.34 mg/g on Mg/Al-hydrochar, 128.20 mg/g on Ca/Al-hydrochar, and 89.29 mg/g on Zn/Al-hydrochar. In addition, layered double hydroxide can be composited with chitosan. Chitosan is known to have the ability as an adsorbent, so it can be used to absorb hazardous materials in some wastewater. According to Barbusiński et al. (2018), chitosan is a natural biopolymer that is well-known and good for water treatment. Chitosan has physical and chemical characteristics, chemical stability, high reactivity, high chelation properties, and high selectivity to pollutants (Seedao et al., 2018).

In present study, a modification of the NiAl LDH composite with chitosan will be carried out. The prepared composite materials were characterized using X-Ray Diffraction (XRD), Fourier Transform Infra-Red (FTIR), and Brunauer Emmet Teller (BET). The resulting composite material will be applied as an adsorbent of organic compounds in the form of phenol. The adsorption parameters to be determined are kinetics, isotherms, and adsorbent regeneration. Determination of the adsorption parameters will be studied through variations in contact time, concentration, and temperature, as well as the desorption process.

## 2. EXPERIMENTAL SECTION

### 2.1 Chemicals and Instrumentation

All chemicals; nickel hexahydrate ($Ni(NO_3)_2.6H_2O$), aluminum nitrate nonahydrate ($Al(NO_3)_3.9H_2O$), sodium carbonate ($Na_2CO_3$), chitosan, hydrogen chloride (HCl), distilled water ($H_2O$), sodium hydroxide (NaOH), phenol ($C_6H_5OH$), 4-aminoantipyrine ($C_{11}H_{13}N_3O$), potassium hexacyanoferrate(III) ($K_3[Fe(CN)_6]$), and acetate buffer solution ($CH_3COO$ Na) pH 10. All instrumentation; X-Ray Diffraction (XRD), spectrophotometer UV-Visible, Brunauer Emmet Teller (BET), and Fourier Transform Infra-Red (FTIR).

### 2.2 Synthesis of NiAl-LDH

A total of 100 mL of a solution containing 0.75 M $Ni(NO_3)_2.6H_2O$ was mixed with 100 mL of a solution containing 0.25 M $Al(NO_3)_3.9H_2O$ and then stirred for 30 min. Furthermore, the pH of the mixture was adjusted to reach pH 10 with the addition of 2 M NaOH. The resulting mixture was then stirred at a temperature of 65°C for 24 h. The samples were filtered and washed with distilled water and then dried in an oven at a temperature of 100°C.

### 2.3 Preparation Chitosan@NiAl LDH

A total of 30 mL of 0.75 M $Ni(NO_3)_2.6H_2O$ were mixed into 30 mL of 0.25 M $Al(NO_3)_2.9H_2O$ solution, then stirred and added 3 gram chitosan. The NaOH solution with a concentration of 2 M was slowly added to the mixture until it reached a pH of 10. Solids were formed after 3 days of stirring at a temperature of 80°C. Then the solid was filtered and washed with distilled water. The composite material obtained was dried at a temperature of 100°C.

### 2.4 Adsorption of Phenol

Adsorption parameters were studied through pH, contact time, concentration, temperature, and regeneration process variations. 0.02 g of adsorbent was put into an Erlenmeyer containing 20 mL of phenol. Adsorption was carried out with variations in pH (2-11), contact time (0-180 min), initial concentration (10-30 mg/L), temperature (30-60°C), and regeneration 5 cycles times. After that, the phenol solution was complex.

The phenol complex process was conducted to Xie et al. (2020) by adding 1 mL of 5 mg/L phenol solution into a beaker. Then 0.1 mL of 2% 4-aminoantipyrine reagent was added, 0.1 mL of hexacyanoferrate (III) 8%, 1 mL of pH 10 buffer solution and 3 mL of distilled water were added. Then the mixture was homogenized and allowed to stand for 5-10 minutes. Afterward, the phenol concentration was measured using a UV-Visible spectrophotometer at 505.2 nm.

## 3. RESULT AND DISCUSSSION

Characterization was carried out using X-rays to produce a NiAl LDH diffractogram, as shown in Figure 1. The results obtained show that there is an angle of 2$\theta$ at 11.57°(003); 22.91°(006); 35.04°(012); 39.73°(015); and 61.9°(110). The success of the NiAl LDH synthesis can be proven by the research of Ahmad et al. (2022) according to JCPDS No.15-0087. The diffraction pattern of chitosan at an angle of 2$\theta$= 7.93° and 19.35°. The 19.35° has a higher intensity than the peak of 7.93°. According to Billah et al. (2020), the angle is 2$\theta$ at= 10° and 20°, indicating that the chitosan material is classified as semi-crystalline by JCPDS data No.039-1894. The results of the characterization of Chitosan@NiAl LDH composites showed that the typical peaks of double-layer hydroxyl were shown at angles of 2$\theta$= 11.45° and 60.93°, while the typical peaks of chitosan were at angles of 2$\theta$= 22.5°.

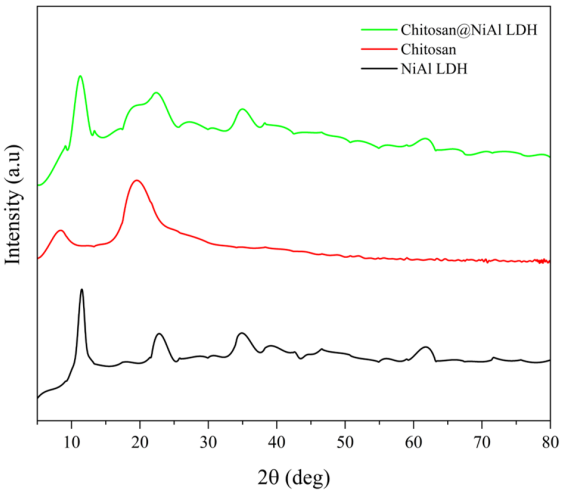


**Figure 1.** X-Ray Diffractogram of Adsorbents

Figure 2 shows the FT-IR spectrum of the Chitosan@NiAl

**Table 1.** Brunauer Emmet Teller of Adsorbents

| Parameter | NiAl LDH | Chitosan | Chitosan@NiAl LDH |
|---|---|---|---|
| Surface Area ($m^2$/g) | 3.288 | 8.558 | 9.493 |
| Pore Volume ($cm^3$/g), BJH | 0.006 | 0.018 | 0.031 |
| Pore Size (nm), BJH | 16.983 | 19.102 | 17.057 |

LDH composite material. Wavenumber 3448 $cm^{-1}$ vibrations occur in the -OH group from water molecules. The O-H bending vibration in the NiAl composite is at a wavenumber of 1635 $cm^{-1}$. The aromatic C=C group derived from chitosan is shown at the wavenumber 1543 $cm^{-1}$. The nitrate group is at a wavenumber of 1543 $cm^{-1}$, and the vibration for metal oxide is at a wavenumber of 601 $cm^{-1}$. According to Cardinale et al. (2020), the NiAl LDH is in the wavenumber region of 3600 $cm^{-1}$. The O-H bonds in each layer are at 1632 $cm^{-1}$. The wavenumber of 1348 $cm^{-1}$ has nitrate groups, and the wavenumbers of 749 and 652 $cm^{-1}$ have metal groups.

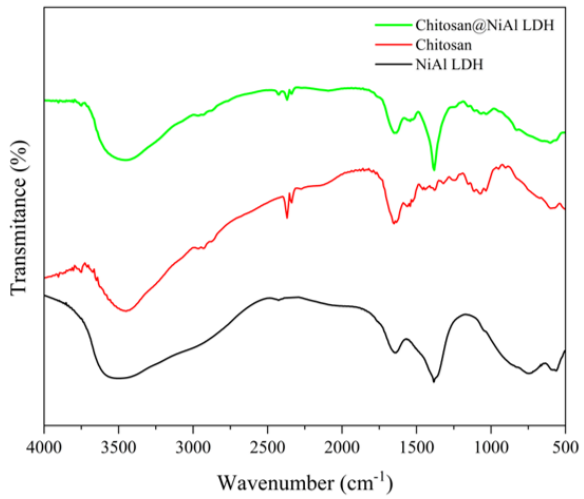


**Figure 2.** Fourier Transfer Infra-Red Spectrum of Adsorbents

The graph nitrogen adsorption-desorption isotherms of NiAl LDH, chitosan, and chitosan@NiAl LDH can be seen in Figure 3. The graph shows that each material belongs to the type IV isotherm based on the classification according to IUPAC. Adsorption can be said to be a type IV isotherm if the adsorbent used has pores in the range of 2-50 nm, and there is an increase in adsorber absorption when the pores are filled with nitrogen (Asnaoui et al., 2022; Cao et al., 2022). The NiAl LDH and chitosan have a surface area of 3.288 $m^2$/g and 8.558 $m^2$/g, respectively. An increase in the surface area of the composite Chitosan@NiAl LDH 9.493 $m^2$/g. Thus, from the data in Table 1, it can be confirmed that the LDH modification process with chitosan material was successfully carried out, characterized by an increase in surface area.

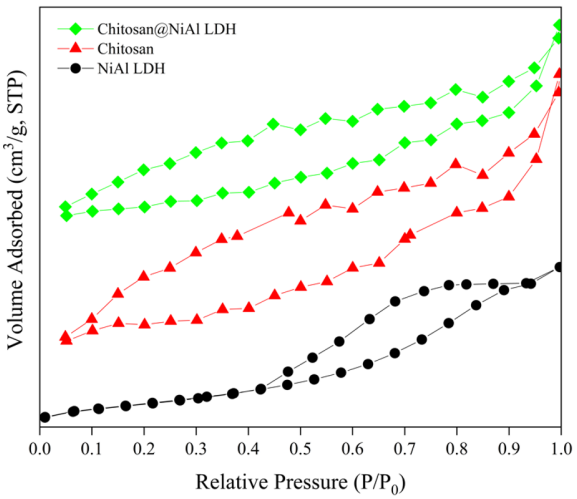


**Figure 3.** Graph Nitrogen Adsorption-Desorption Isotherms of Adsorbents

The effect of pH plays an essential role in the adsorption process (Qu et al., 2022). Figure 4 shows the optimum pH of the NiAl LDH at pH 3, with the adsorbed concentration reaching 13.355 mg/L. The optimum pH for chitosan and chitosan@NiAl LDH material is at the optimum pH of 5, with the adsorbed chitosan concentration of 10.414 mg/L, while chitosan@NiAl LDH of 14.663 mg/L. According to Al-Ghouti et al. (2022), when the solution's pH is smaller or in an acidic solution state, the graphite oxide is positively charged, while in an alkaline solution or an alkaline solution, the surface of adsorbent is negatively charged. Therefore, the efficiency of phenol adsorption decreases at alkaline pH conditions; this is due to the electrostatic repulsion between phenol and the negatively charged surface of graphite oxide.

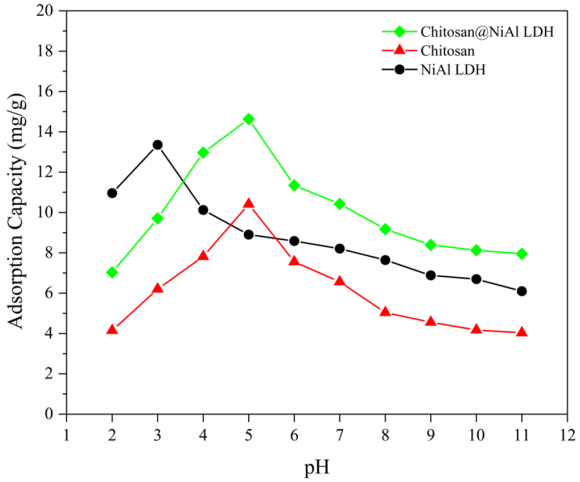


**Figure 4.** Effect of pH on Adsorption of Phenol

**Table 2.** Pseudo-First Order and Pseudo-Second Order Parameter

| Adsorbents | $Qe_{exp}$ (mg/g) | PFO $Qe_{calc}$ (mg/g) | PFO $k_1$ ($min^{-1}$) | PFO $R^2$ | PSO $Qe_{calc}$ (mg/g) | PSO $k_2$ (g/mg.min) | PSO $R^2$ |
|---|---|---|---|---|---|---|---|
| NiAl LDH | 12.274 | 7.224 | 0.030 | 0.9719 | 12.804 | 0.010 | 0.9997 |
| Chitosan | 9.774 | 7.511 | 0.029 | 0.9452 | 10.311 | 0.008 | 0.9967 |
| Chitosan@NiAl LDH | 13.722 | 14.997 | 0.048 | 0.8676 | 14.556 | 0.007 | 0.9987 |

**Table 3.** Langmuir and Freundlich Parameter

| Adsorbent | T (°C) | Langmuir $Q_{max}$ | Langmuir kL | Langmuir $R^2$ | Freundlich n | Freundlich kF | Freundlich $R^2$ |
|---|---|---|---|---|---|---|---|
| NiAl LDH | 30 | 25.445 | 0.438 | 0.845 | 1.395 | 1.456 | 0.9478 |
| | 40 | 25.063 | 0.055 | 0.8827 | 1.466 | 1.801 | 0.9447 |
| | 50 | 23.041 | 0.079 | 0.9392 | 1.653 | 2.469 | 0.9516 |
| | 60 | 24.155 | 0.088 | 0.9451 | 1.685 | 2.820 | 0.9548 |
| Chitosan | 30 | 23.753 | 0.026 | 0.6276 | 1.270 | 6.703 | 0.9292 |
| | 40 | 22.472 | 0.031 | 0.5671 | 1.295 | 2.078 | 0.8803 |
| | 50 | 20.704 | 0.041 | 0.6888 | 1.362 | 4.248 | 0.8859 |
| | 60 | 17.668 | 0.064 | 0.8866 | 1.581 | 7.579 | 0.9074 |
| Chitosan@NiAl LDH | 30 | 29.851 | 0.037 | 0.662 | 1.366 | 1.472 | 0.9343 |
| | 40 | 32.468 | 0.040 | 0.8074 | 1.348 | 1.652 | 0.9645 |
| | 50 | 33.223 | 0.044 | 0.8483 | 1.357 | 1.828 | 0.9687 |
| | 60 | 26.596 | 0.076 | 0.9052 | 1.609 | 2.685 | 0.9654 |

Pseudo-first order and pseudo-second order were used to determine the adsorption rate using the results of the data on the effect of phenol adsorption time in Figure 5. The kinetic model in the adsorption process can be determined by looking at the value of the coefficient of determination ($R^2$) which is close to 1, the smallest value of the kinetic rate (k), and the similarity between the experimental Qe value and the calculated Qe. Based on Table 2, all adsorbent materials follow the pseudo-second-order kinetic model. This can be proven by the data of the coefficient of determination ($R^2$) which is close to 1, and the value of the kinetic rate ($k_2$) in the pseudo-second-order kinetic model is smaller than the value of the pseudo-first-order kinetic rate ($k_1$), so it can be concluded that the reaction proceeds faster in the model pseudo-second order kinetics. Pseudo-second order implied adsorption of phenol was chemisorption (Gao et al., 2022).

The Langmuir isotherm equation is used if the adsorption process is in the form of a single layer or monolayer and there is an interaction between the adsorbate molecules. The Freundlich isotherm equation applies to adsorption processes that occur in several layers or multilayers so that there is no association and dissociation of the adsorbate molecules (Liu et al., 2021). The results of the NiAl LDH, chitosan, and chitosan@NiAl LDH adsorption isotherm data can be seen in Table 3. All adsorbents followed the Freundlich equation adsorption isotherm model, seeing the correlation coefficient ($R^2$) value closer to the value of 1. The maximum adsorption capacity of NiAl LDH, chitosan, and chitosan@NiAl LDH is 25.445, 23.753, and 33.223 mg/g, respectively. Comparison maximum capacities this work with other research in adsorption shown in Table 4.

**Table 4.** Comparison Maximum Capacities Adsorption of Phenol with Other Research

| Adsorbent | $Q_{max}$ (mg/g) | Reference |
|---|---|---|
| Bentonite | 23.64 | (Ahmadi and Igwegbe, 2018) |
| $\alpha$-$Fe_2O_3$ | 21.93 | (Dehmani et al., 2020) |
| Clarified sludge | 1.052 | (Mandal and Das, 2019) |
| SWNTO | 30.864 | (De la Luz-Asunción et al., 2015) |
| GEO | 28.986 | (De la Luz-Asunción et al., 2015) |
| Lignite | 6.216 | (Liu et al., 2021) |
| Natural Clay | 10.1 | (Dehmani et al., 2021a) |
| $ZnCl_2$-BFAC | 17.02 | (Sathya Priya and Sureshkumar, 2020) |
| Tea waste | 7.62 | (Gupta and Balomajumder, 2015) |
| $Zn_4$Al-LDH | 7.73 | (Lupa et al., 2018) |
| NiAl LDH | 25.445 | This work |
| Chitosan | 23.753 | This work |
| Chitosan@NiAl LDH | 33.223 | This work |

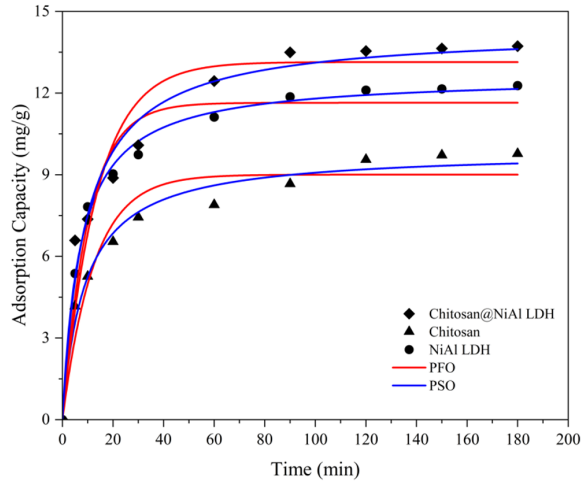


**Figure 5.** Pseudo-First Order and Pseudo-Second Order for Adsorption of Phenol

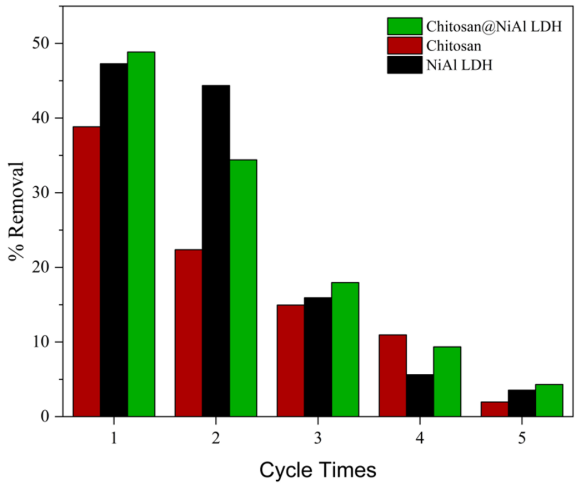


**Figure 6.** Regeneration Study of Adsorbent

Based on Figure 6, it can be seen that the adsorbent regeneration process decreased during the third regeneration. The percentage of phenol adsorbed using NiAl LDH, chitosan, and chitosan@NiAl LDH during the first regeneration reached 47.821, 38.844, 48.859%, respectively. The increase in regeneration cycles causes a decrease in the percentage of adsorbed; sequentially, the percentage adsorbed during the fifth regeneration reaches 3.545, 1.966, 4.309%, respectively.

## 4. CONCLUSION

Modification of the NiAl LDH composite with chitosan was successful by characterization XRD, FTIR and BET. The optimum pH of the NiAl LDH at pH 3, the optimum pH for chitosan and chitosan@NiAl LDH material is pH 5. The kinetic and isotherm model in the adsorption process is pseudo-second-order and Freundlich model, respectively. The maximum adsorption capacity of NiAl LDH, chitosan, and chitosan@NiAl LDH is 25.445, 23.753, and 33.223 mg/g, respectively. The increase in regeneration cycles causes a decrease in the percentage of adsorbed; sequentially, the percentage adsorbed during the fifth regeneration reaches 3.545, 1.966, 4.309%, respectively.

## 5. ACKNOWLEDGMENT

The authors thank the Research Centre of Inorganic Materials and Coordination Complexes FMIPA Universitas Sriwijaya for support and instrumental analysis.

## REFERENCES

Ahmad, N., A. Wijaya, Amri, E. S. Fitri, F. S. Arsyad, R. Mohadi, and A. Lesbani (2022). Catalytic Oxidative Desulfurization of Dibenzothiophene by Composites Based Ni/Al-Oxide. *Science and Technology Indonesia*, **7**(3); 385–91

Ahmadi, S. and C. A. Igwegbe (2018). Adsorptive Removal of Phenol and Aniline by Modified Bentonite: Adsorption Isotherm and Kinetics Study. *Applied Water Science*, **8**(6); 1–8

Al-Ghouti, M. A., J. Sayma, N. Munira, D. Mohamed, D. A. Da'na, H. Qiblawey, and A. Alkhouzaam (2022). Effective Removal of Phenol from Wastewater using a Hybrid Process of Graphene Oxide Adsorption and UV-Irradiation. *Environmental Technology & Innovation*, **27**; 102525

Alves, D. C., J. O. Goncalves, B. B. Coseglio, T. A. Burgo, G. L. Dotto, L. A. Pinto, and T. R. Cadaval Jr (2019). Adsorption of Phenol Onto Chitosan Hydrogel Scaffold Modified with Carbon Nanotubes. *Journal of Environmental Chemical Engineering*, **7**(6); 103460

Asnaoui, H., Y. Dehmani, M. Khalis, and E. K. Hachem (2022). Adsorption of Phenol from Aqueous Solutions by Na–Bentonite: Kinetic, Equilibrium and Thermodynamic Studies. *International Journal of Environmental Analytical Chemistry*, **102**(13); 3043–3057

Barbusiński, K., S. Salwiczek, and A. Paszewska (2018). The Use of Chitosan for Removing Selected Pollutants from Water and Wastewater–Short Review. *Architecture, Civil Engineering, Environment*, **9**(2); 107-115

Billah, R. E. K., Y. Abdellaoui, Z. Anfar, G. Giácoman-Vallejos, M. Agunaou, and A. Soufiane (2020). Synthesis and Characterization of Chitosan/Fluorapatite Composites for the Removal of Cr(VI) from Aqueous Solutions and Optimized Parameters. *Water, Air, & Soil Pollution*, **231**(4); 1–14

Bouteraa, S., F. B. D. Saiah, S. Hamouda, and N. Bettahar (2020). Zn-M-$CO_3$ Layered Double Hydroxides (M= Fe, Cr, or Al): Synthesis, Characterization, and Removal of Aqueous Indigo Carmine. *Bulletin of Chemical Reaction Engineering & Catalysis*, **15**; 43–54

Cao, Y., Y. Wang, F. Zhou, J. Huang, and M. Xu (2022). Acylamino-Functionalized Hyper-Cross-Linked Polymers for Efficient Adsorption Removal of Phenol in Aqueous Solution. *Separation and Purification Technology*; 122229

 

Cardinale, A. M., C. Carbone, S. Consani, M. Fortunato, and N. Parodi (2020). Layered Double Hydroxides for Remediation of Industrial Wastewater from a Galvanic Plant. *Crystals*, **10**(6); 443

da Silva, M. C., C. Schnorr, S. F. Lütke, S. Knani, V. X. Nascimento, É. C. Lima, P. S. Thue, J. Vieillard, L. F. Silva, and G. L. Dotto (2022). KOH Activated Carbons from Brazil Nut Shell: Preparation, Characterization, and their Application in Phenol Adsorption. *Chemical Engineering Research and Design*, **187**; 387–396

de Farias, M. B., P. Prediger, and M. G. A. Vieira (2022). Conventional and Green-Synthesized Nanomaterials Applied for the Adsorption and/or Degradation of Phenol: A Recent Overview. *Journal of Cleaner Production*; 132980

De la Luz-Asunción, M., V. Sánchez-Mendieta, A. Martínez-Hernández, V. Castaño, and C. Velasco-Santos (2015). Adsorption of Phenol from Aqueous Solutions by Carbon Nanomaterials of One and Two Dimensions: Kinetic and Equilibrium Studies. *Journal of Nanomaterials*, **2015**

Dehmani, Y., A. A. Alrashdi, H. Lgaz, T. Lamhasni, S. Abouarnadasse, and I. M. Chung (2020). Removal of Phenol from Aqueous Solution by Adsorption onto Hematite ($\alpha$-$Fe_2O_3$): Mechanism Exploration from Both Experimental and Theoretical Studies. *Arabian Journal of Chemistry*, **13**(5); 5474–5486

Dehmani, Y., O. El Khalki, H. Mezougane, and S. Abouarnadasse (2021a). Comparative Study on Adsorption of Cationic Dyes and Phenol by Natural Clays. *Chemical Data Collections*, **33**; 100674

Dehmani, Y., H. Lgaz, A. A. Alrashdi, T. Lamhasni, S. Abouarnadasse, and I. M. Chung (2021b). Phenol Adsorption Mechanism on the Zinc Oxide Surface: Experimental, Cluster DFT Calculations, and Molecular Dynamics Simulations. *Journal of Molecular Liquids*, **324**; 114993

Gao, W., Z. Lin, H. Chen, S. Yan, H. Zhu, H. Zhang, H. Sun, S. Zhang, S. Zhang, and Y. Wu (2022). Roles of Graphitization Degree and Surface Functional Groups of N-Doped Activated Biochar for Phenol Adsorption. *Journal of Analytical and Applied Pyrolysis*, **167**; 105700

Gupta, A. and C. Balomajumder (2015). Simultaneous Removal of Cr(VI) and Phenol from Binary Solution using *Bacillus sp.* Immobilized onto Tea Waste Biomass. *Journal of Water Process Engineering*, **6**; 1–10

Jain, M., S. A. Khan, A. Sahoo, P. Dubey, K. K. Pant, Z. M. Ziora, and M. A. Blaskovich (2022). Statistical Evaluation of Cow-Dung Derived Activated Biochar for Phenol Adsorption: Adsorption Isotherms, Kinetics, and Thermodynamic Studies. *Bioresource Technology*, **352**; 127030

Juleanti, N., N. Normah, P. M. S. B. N. Siregar, A. Wijaya, N. R. Palapa, T. Taher, N. Hidayati, R. Mohadi, and A. Lesbani (2022). Comparison of the Adsorption Ability of MgAl-HC, CaAl-HC, and ZaAl-HC Composite Materials Based on Duku Peel Hydrochar in Adsorption of Direct Green Anionic Dyes. *Indonesian Journal of Chemistry*, **22**(1); 192–204

Khan, D., J. Kuntail, and I. Sinha (2022). Mechanism of Phenol and p-Nitrophenol Adsorption on Kaolinite Surface in Aqueous Medium: A Molecular Dynamics Study. *Journal of Molecular Graphics and Modelling*; 108251

Lesbani, A., N. R. Palapa, R. J. Sayeri, T. Taher, and N. Hidayati (2021). High Reusability of NiAl LDH/Biochar Composite in the Removal Methylene Blue from Aqueous Solution. *Indonesian Journal of Chemistry*, **21**(2); 421–434

Liu, X., Y. Tu, S. Liu, K. Liu, L. Zhang, G. Li, and Z. Xu (2021). Adsorption of Ammonia Nitrogen and Phenol onto the Lignite Surface: An Experimental and Molecular Dynamics Simulation Study. *Journal of Hazardous Materials*, **416**; 125966

Lupa, L., L. Cocheci, R. Pode, and I. Hulka (2018). Phenol Adsorption using Aliquat 336 Functionalized Zn-Al Layered Double Hydroxide. *Separation and Purification Technology*, **196**; 82–95

Mandal, A. and S. K. Das (2019). Phenol Adsorption from Wastewater using Clarified Sludge from Basic Oxygen Furnace. *Journal of Environmental Chemical Engineering*, **7**(4); 103259

Qu, Y., L. Qin, X. Liu, and Y. Yang (2022). Magnetic $Fe_3O_4$/ZIF-8 Composite as an Effective and Recyclable Adsorbent for Phenol Adsorption from Wastewater. *Separation and Purification Technology*, **294**; 121169

Sathya Priya, D. and M. Sureshkumar (2020). Synthesis of Borassus Flabellifer Fruit Husk Activated Carbon Filter for Phenol Removal from Wastewater. *International Journal of Environmental Science and Technology*, **17**(2); 829–842

Seedao, C., T. Rachphirom, M. Phiromchoei, and W. Jangiam (2018). Anionic Dye Adsorption from Aqueous Solutions by Chitosan Coated Luffa Fibers. *ASEAN Journal of Chemical Engineering*, **18**(2); 31–40

Taher, T., R. Putra, N. R. Palapa, and A. Lesbani (2021). Preparation of Magnetite-Nanoparticle-Decorated NiFe Layered Double Hydroxide and its Adsorption Performance for Congo Red Dye Removal. *Chemical Physics Letters*, **777**; 138712

Wang, P., X. Geng, L. Luo, Y. Liu, R. I. Eglitis, and X. Wang (2022). The Adsorption Behavior of Phenol on the Surface of 1D/2D M@MoS2 (M= Co and Rh) for Hydrodeoxidation Reaction: Insights from Theoretical Investigations. *Applied Surface Science*, **601**; 154242

Xie, B., J. Qin, S. Wang, X. Li, H. Sun, and W. Chen (2020). Adsorption of Phenol on Commercial Activated Carbons: Modelling and Interpretation. *International Journal of Environmental Research and Public Health*, **17**(3); 789

Zhang, J., N. Liu, H. Gong, Q. Chen, and H. Liu (2022). Hydroxyl-Functionalized Hypercrosslinked Polymers with Ultrafast Adsorption Rate as an Efficient Adsorbent for Phenol Removal. *Microporous and Mesoporous Materials*, **336**; 111836

 